

reduction have similar structures and exhibit a similar dynamic behavior as the corresponding galvinoxyl radicals which are generated by oxidation of the parent galvinoxyls. On the other hand, the spin density distributions in these two types of radicals are completely different. This allows the investigation of different properties. Thus, phenyl hyperconjugation can be studied in ortho-substituted triphenylmethyl-type radicals whereas the phenyl proton coupling constants in the respective galvinoxyls are too small for this purpose. Moreover, the mechanism of spin density transfer into alkyl groups can be investigated in diphenylmethyl-type radicals because of the large spin population at the central carbon atom. In this context, the potential of the general TRIPLE method for a determination of signs of hyperfine coupling constants proved to be of great value.

**Acknowledgment.** We thank Dr. K. Schubert and M. Sordo for samples of the  $^{13}\text{C}$ -labeled and deuterated galvinoxyls, respectively. H. K. gratefully acknowledges financial support by Deutsche Forschungsgemeinschaft (Normalverfahren) and Fonds der Chemischen Industrie. B. K. gratefully acknowledges a Liebig stipend of the Fonds der Chemischen Industrie.

**Registry No.** 1a, 2887-52-7; 1b, 93403-31-7; 1d, 93403-32-8; 2a, 56523-92-3; 2b, 93425-33-3; 3a, 93403-33-9; 3b, 93403-34-0; 4a, 93425-34-4; 4b, 93425-35-5; 5a, 61937-92-6; 5b, 93425-36-6; 6a, 74853-85-3; 6b, 93403-35-1; 7a, 79320-49-3; 7b, 93403-36-2; 8a, 79320-50-6; 8b, 93403-37-3; 9a, 61937-90-4; 9b, 93403-38-4; 10a, 93403-39-5; 10b, 93403-40-8; (2,6-di-*tert*-butyl-4-bromophenoxy)trimethylsilane, 27329-74-4; 2,4,6-trimethylbenzoic acid methyl ester, 2282-84-0; triphenylmethyl, 2216-49-1; sodium amalgam, 11110-52-4.

## Two-Dimensional NMR Spectroscopy of Tetra-*o*-tolylcyclopentadienone. Complete Rotamer Assignment

Rudolph Willem,<sup>\*1</sup> Arnold Jans,<sup>2</sup> Cornelis Hoogzand,<sup>1</sup> Marcel Gielen,<sup>1</sup> Georges Van Binst,<sup>2</sup> and Henri Pepermans<sup>1,3</sup>

Contribution from the Vrije Universiteit Brussel, AOSC-TW, Pleinlaan 2, B-1050 Brussel, Belgium. Received June 13, 1984

**Abstract:** A slow-exchange 2D NMR experiment on tetra-*o*-tolylcyclopentadienone allows the making of a complete rotamer assignment and leads to stronger experimental evidence to the uncorrelated rotation of the *o*-tolyl rings in the  $\alpha$  position as the threshold mode.

Recently we presented a detailed  $^1\text{H}$  and  $^{13}\text{C}$  NMR study on the stereochemistry of tetra-*o*-tolylcyclopentadienone (compound 1).<sup>4</sup> We proposed a static stereochemistry, based on a molecular framework, in which the four peripheral *o*-tolyl rings are perpendicular to the central cyclopentadienone ring, at least on the NMR time scale. Thus compound 1 exists as a mixture of ten rotamers. Their characteristics are given in Table I and in Table I of ref 4. Therefore, a total of 16 methyl resonances is expected, in achiral solvents<sup>4</sup> when internal rotations are frozen out, 8 being due to the  $\alpha$  *o*-tolyl rings and the 8 others to the  $\beta$  ones.

In the  $^1\text{H}$  spectra recorded in the slow-exchange region of 1 ( $-60$  to  $-30$  °C), we observed at most 14 signals, with important overlapping or tailing. It was, therefore, impossible to make any assignments of these signals to the rotamers they arise from; neither we could assert whether two signals are missing because of accidental isochronies or because one of the rotamers is much less populated than the others.<sup>4</sup>

In a medium-temperature range, we observed four residual<sup>5-7</sup> methyl signals, two almost isochronous low-field  $\alpha$  ones and two

high field  $\beta$  ones, assignable to two residual isomers.<sup>4</sup> This partial coalescence is due to internal rotations of *o*-tolyl rings becoming rapid on the NMR time scale. This behavior was shown to be compatible with only four out of the ten possible modes of internal rotations of 1: two three-ring rotations,  $M_7$  and  $M_8$ , and two one-ring rotations,  $M_1$  (the  $\alpha$  one ring rotation) and  $M_2$  (the  $\beta$  one ring rotation). We excluded  $M_7$  and  $M_8$ , though NMR indistinguishable from  $M_2$  and  $M_1$ , respectively, for steric reasons. We preferred  $M_1$  as the threshold mode rather than  $M_2$  exclusively on the basis of qualitative activation barrier considerations.<sup>4</sup>

The aim of this paper is to propose a complete rotamer assignment together with strong two-dimensional NMR evidence for the  $\alpha$  one-ring rotation as the threshold mode.

Figure 1 presents the methyl region of a resolution-enhanced<sup>4,8,9</sup> (Lorentz-Gauss) 500-MHz  $^1\text{H}$  spectrum, recorded in  $\text{CDCl}_3$  at  $-43$  °C, with our signal numbering, our rotamer assignment, and the constitution  $\alpha$  or  $\beta$  of the methyl group that the signal arises from (see also Table I). Signals with double numbering are pairs of isochronous resonances (see below).

The 500-MHz spectrum of Figure 1 compared fairly well with the 270-MHz spectrum at  $-40$  °C of Figure 4 of ref 4 except for two details: (1) the well-separated signals 9 and 10 in the 500-MHz spectrum are isochronous in the 270-MHz spectrum of ref 4; and (2) the two isochronous signals 15 and 16 in the 500-MHz spectrum at  $-43$  °C are well separated in the 270-MHz spectrum at  $-40$  °C. We attribute the latter observation to a strong temperature dependence of the chemical shift of signal 15.

Figure 2 represents identical contour plots of the slow-exchange 500-MHz 2D spectrum, recorded at  $-43$  °C, to which we have superimposed the networks, indicating, respectively, which  $\alpha$  and

(1) Dienst voor Algemene en Organische Scheikunde, Fakulteit Toegepaste Wetenschappen.

(2) Eenheid Organische Chemie en Instrumentele Eenheid, Fakulteit Wetenschappen.

(3) Aspirant at the Belgian Nationaal Fonds voor Wetenschappelijk Onderzoek (NFWO).

(4) Willem, R.; Pepermans, H.; Hoogzand, C.; Hallenga, K.; Gielen, M. *J. Am. Chem. Soc.* **1981**, *103*, 2297.

(5) (a) Finocchiaro, P.; Gust, D.; Mislow, K. *J. Am. Chem. Soc.* **1974**, *96*, 3205. (b) Finocchiaro, P.; Hounshell, W. D.; Mislow, K. *J. Am. Chem. Soc.* **1976**, *98*, 4952. (c) Mislow, K. *Acc. Chem. Res.* **1976**, *9*, 26 and references cited therein.

(6) Brocas, J.; Gielen, M.; Willem, R. "The Permutational Approach to Dynamic Stereochemistry"; McGraw-Hill: New York, 1983; pp 399-400, 503 and references cited therein.

(7) (a) Aue, W. P.; Bartholdi, E.; Ernst, R. R. *J. Chem. Phys.* **1976**, *64*, 2229. Jeener, J.; Meier, B. H.; Bachmann, D.; Ernst, R. R. *J. Chem. Phys.* **1979**, *71*, 4546. (c) Meier, B. H.; Ernst, R. R. *J. Am. Chem. Soc.* **1979**, *101*, 6441.

(8) (a) Willem, R.; Pepermans, H.; Hallenga, K.; Gielen, M.; Dams, R.; Geise, H. J. *J. Org. Chem.* **1983**, *48*, 1890. (b) Ernst, R. R. *Adv. Magn. Reson.* **1968**, *2*, 1. (c) Ferrige, A. G.; Lindon, J. C. *J. Magn. Reson.* **1978**, *31*, 337. (d) Hallenga, K.; Ressler, F., unpublished results.

(9) Hull, W. E.; Bruker, Two-Dimensional NMR, aspect 2000-3000, 1982.

Table I. Rotamers of 1<sup>a</sup>

rotamer	point group	signal assignment		$\sigma_r$	$m_r$	$n_r^{\alpha\beta\text{cis}}$	$n_r^{\beta\beta\text{cis}}$	$x_r P(x,y)$	$x_r^{\text{exptl}}$	$x_r^{\text{calcd}}$	
		$\alpha$	$\beta$							$M_1$	$M_2$
I <sub>1</sub>	C <sub>s</sub>	9	6	1	1	2	1	$z^2y$	0.04	0.05	0.07
I <sub>2</sub> /I <sub>2</sub>	C <sub>1</sub>	2, 16	8, 11	1	2	1	1	$2zy$	0.16	0.17	0.23
I <sub>3</sub>	C <sub>s</sub>	1	10	1	1	0	1	$y$	0.13	0.13	0.19
I <sub>4</sub> /I <sub>4</sub>	C <sub>2</sub>	7	15	2	2	2	0	$z^2$	0.13	0.09	0.07
I <sub>5</sub> /I <sub>5</sub>	C <sub>1</sub>	3, 5	12, 14	1	2	1	0	$2z$	0.28	0.31	0.24
I <sub>6</sub> /I <sub>6</sub>	C <sub>2</sub>	4	13	2	2	0	0	1	0.26	0.25	0.20

<sup>a</sup> Point groups, signal assignment, algebraic expression of the populations together with their experimental values and the calculated ones assuming the modes  $M_1$  and  $M_2$ .  $\sigma_r$  = symmetry number of rotamer  $r$ ;  $m_r$  = mixing entropy factor;  $n_r^{\alpha\beta\text{cis}}$  = number of  $\alpha\beta$  cis interactions in rotamer  $r$ ;  $n_r^{\beta\beta\text{cis}}$  = number of  $\beta\beta$  cis interactions in rotamer  $r$ .

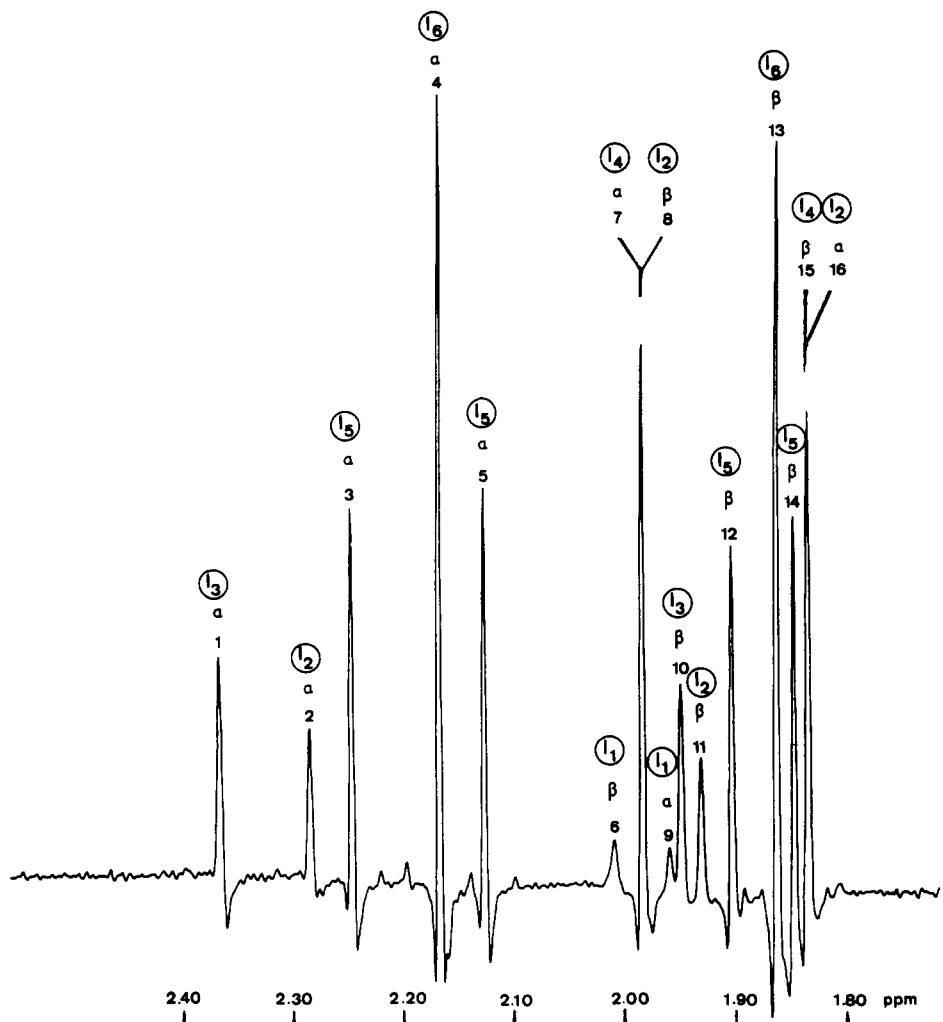


Figure 1. Resolution-enhanced 1D NMR spectrum at 500 MHz of 1, in the methyl region, at -43 °C in CDCl<sub>3</sub>.

$\beta$  signals exchange their magnetization. In ideal experimental circumstances, such a 2D spectrum is a faithful representation of the Kubo-Sack matrix<sup>6</sup> of magnetic site exchanges. The contours of the main diagonal represent cross sections of the 1D spectrum at chosen levels. The nondiagonal contours, the so-called cross peaks, at the coordinates  $ij$  and  $ji$  indicate a magnetization transfer from the site with chemical shift  $\delta_i$  to the one with chemical shift  $\delta_j$  and conversely.

The cross peaks of the 2D spectrum of 1 have intensities, depending on the rate constants of magnetization transfers. These constants are different because the isomerizations occur between rotamers with different energies. Therefore, the cross peak intensities are different, in particular also those of a pair  $ij$  and  $ji$ . In practice, however, we have chosen to symmetrize the cross peaks with respect to the main diagonal, with reference to the less intense one, in order to avoid the strong artifacts due to the axial peaks.<sup>7</sup> Therefore, no quantitative information can be obtained from these contours. Moreover, for high contour levels, some weak but

relevant cross peaks can be missing.

The argumentation for the construction of the networks  $\alpha$  and  $\beta$  of Figure 2 is the following. Our previous stereochemical analysis<sup>4</sup> (see Figures 8 and 9 to ref 4) shows that for both the modes  $M_1$  and  $M_2$ , the graphs representing the magnetic site exchanges are composed of four square subgraphs; there are two such subgraphs for the  $\alpha$  resonances and two for the  $\beta$  ones. The four signals associated with each subgraph coalesce to a unique residual signal. The square structure of these subgraphs indicates that each magnetic site can be transferred to precisely two others when the internal rotations of  $M_1$  or  $M_2$  do proceed. As a consequence the magnetic site exchange matrices associated with such a subgraph must each exhibit two nonzero nondiagonal elements on each row and column. As a result, four submatrices, having each two cross peaks on each row and column, must appear in the 2D spectrum. The networks of Figure 2 show that this is actually the case. The four magnetic site exchange submatrices deduced from the 2D spectrum are the following:

		1	2	9	16			3	4	5	7
$\alpha^1 =$	1	0	1	0	1		3	0	1	0	1
	2	1	0	1	0		4	1	0	1	0
	9	0	1	0	1		5	0	1	0	1
	16	1	0	1	0		7	1	0	1	0

		6	8	10	11			12	13	14	15
$\beta^1 =$	6	0	1	0	1		12	0	1	0	1
	8	1	0	1	0		13	1	0	1	0
	10	0	1	0	1		14	0	1	0	1
	11	1	0	1	0		15	1	0	1	0

In these submatrices the row and column indexes represent the methyl signals. A nondiagonal  $\alpha_{ij}$  or  $\beta_{ij}$  element is equal to 1 when the entry  $ij$  of the 2D spectrum exhibits a cross peak and is equal to 0 otherwise. For commodity, the diagonal contours have been set equal to 0 since they are irrelevant to the analysis of the magnetic site exchange. In practice, small differences between the expected and the experimental 2D spectrum are observed. Contours which do not lie at the intersection of rows and columns are artifacts. Further, the pair of small cross peaks appearing at the coordinates 47/74, not indicated in the matrix  $\alpha^2$ , is attributed to a two-step magnetization transfer. Note moreover that the matrix elements  $\beta^1_{68}$  and  $\beta^1_{86}$  equal to 1 in the matrix  $\beta^1$ , do not appear in the 2D spectrum of Figure 2. We observed them, however, in 2D spectra not shown here which have a lower contour level or which were recorded with longer mixing times, but these spectra displayed also more artifacts. The same remark holds for the pair of elements  $\beta^1_{10,11}$  and  $\beta^1_{11,10}$  which do appear only as tails in Figure 2. The cross peaks associated with the pair of matrix elements  $\beta^2_{12,15}$  and  $\beta^2_{15,12}$  lie in fact between the rows and columns 14 and 15.

To our opinion this reflects a little temperature instability in the NMR probe since the 1D spectra showed that signal 15 is very sensitive to the temperature. Moreover the exact position of signal 15 on the main diagonal of the 2D spectrum is made a little uncertain by its overlapping with signal 16.

The symbol  $\alpha$  or  $\beta$  of the matrix indicates whether it describes four magnetic site exchanges of  $\alpha$  or  $\beta$  sites. The assignment of the submatrices to  $\alpha$  or  $\beta$  sites can be made from a chemical shift argument. The signals of the submatrices  $\beta^1$  and  $\beta^2$  coalesce to residual signals at, respectively, 1.99 and 1.88 ppm at 30 °C in  $\text{CDCl}_3$  and correspond fairly well with those observed at 2.04 and 1.90 ppm for 3,4-di-*o*-tolyl-2,5-diphenylcyclopentadienone<sup>10</sup> (compound 2) in which only  $\beta$  and no  $\alpha$  *o*-tolyl rings are present. Moreover, these two residual signals coalesce in turn at higher temperatures (Figure 7 of ref 4). For these reasons we identify these two sets of high field signals (6,8,10,11 and 12–15) as  $\beta$  signals. The signals of the submatrices  $\alpha^1$  and  $\alpha^2$  coalesce to two accidentally isochronous residual signals at 2.14 ppm; this resonance is of course absent in 2.<sup>10</sup> Therefore, we identify these two sets of signals (1,2,9,16 and 3–7) as  $\alpha$  ones. The wider range in the chemical shift of the  $\alpha$  signals is attributed both to a larger variation in the torsion angles of the  $\alpha$  rings with respect to the  $\beta$  ones and to the magnetic anisotropy of the carbonyl ring lying closer to the  $\alpha$  than to the  $\beta$  ones.

Starting now from this identification and from the basic idea that for a given rotamer there are equal numbers of  $\alpha$  and  $\beta$  resonances with identical intensities, we can now attribute all these signals to the rotamers they arise from. To do so, we evaluate the populations of the rotamers (or pairs of enantiomeric ones) by using a model developed recently by Pepermans<sup>11</sup> which was applied successfully to the attribution of the rotamers of hexarylbenzenes. This model allows the computation of the populations of the rotamers parametrically as a function of the number of cis and trans interactions between the *o*-tolyl rings. With the cis (respectively trans) interaction, we mean the interaction between two neighboring *o*-tolyl rings on which the methyl groups lie on the same side (respectively the opposite side) of the cy-

clopentadienone ring. In 1 there are two  $\alpha\beta$  interactions and one  $\beta\beta$  interaction, each of which can be either cis or trans. Assuming that in the first approximation, the population differences between the rotamers are only due to differences between their symmetry entropies and their enantiomer mixing entropies and are due to the free enthalpy contributions resulting from the above  $\alpha\beta$  and  $\beta\beta$  interactions, the number of moles of rotamer  $r$  at equilibrium can be expressed as

$$N_r = \gamma \frac{m_r}{\sigma_r} \exp \left\{ -\frac{1}{RT} [n_r^{\alpha\beta\text{cis}} G^{\alpha\beta\text{cis}} + n_r^{\alpha\beta\text{trans}} G^{\alpha\beta\text{trans}} + n_r^{\beta\beta\text{cis}} G^{\beta\beta\text{cis}} + n_r^{\beta\beta\text{trans}} G^{\beta\beta\text{trans}}] \right\} \quad (1)$$

In formula 1,  $m_r = 1$  or 2 according to whether the rotamer  $r$  is achiral or chiral, so that we can treat a pair of enantiomeric rotamers as a single rotamer. The constant  $\sigma_r$  represents the symmetry number of rotamer  $r$ . The term  $G^{\alpha\beta\text{cis}}$  represents the contribution to the free enthalpy due to one  $\alpha\beta$  cis interaction and is supposed to be the same for all the rotamers;  $n_r^{\alpha\beta\text{cis}}$  represents the number of times this interaction appears in rotamer  $r$ . The quantities  $G^{\alpha\beta\text{trans}}$ ,  $G^{\beta\beta\text{cis}}$ , and  $G^{\beta\beta\text{trans}}$  on one hand and  $n_r^{\alpha\beta\text{trans}}$ ,  $n_r^{\beta\beta\text{cis}}$ , and  $n_r^{\beta\beta\text{trans}}$  on the other hand are defined analogously. The proportionality factor  $\gamma$  is supposed to be independent of rotamer  $r$ . Taking into account that

$$n_r^{\alpha\beta\text{cis}} + n_r^{\alpha\beta\text{trans}} = 2$$

and

$$n_r^{\beta\beta\text{cis}} + n_r^{\beta\beta\text{trans}} = 1$$

and defining

$$z = \exp \left[ -\frac{1}{RT} (G^{\alpha\beta\text{cis}} - G^{\alpha\beta\text{trans}}) \right]$$

and

$$y = \exp \left[ -\frac{1}{RT} (G^{\beta\beta\text{cis}} - G^{\beta\beta\text{trans}}) \right]$$

the molar population of rotamer  $r$  at equilibrium can be calculated from eq 1 to be

$$x_r = \frac{N_r}{\sum_r N_r} = \frac{m_r}{\sigma_r} \frac{z^{n_r^{\alpha\beta\text{cis}}} y^{n_r^{\beta\beta\text{cis}}}}{P(z,y)} \quad (2)$$

where  $P(z,y) = (z+1)^2(y+1)$ .

Using the data of Table I of ref 4, we calculate with eq 2 the mathematical expressions of rotamer populations, as a function of  $z$  and  $y$ , since  $m_r$ ,  $\sigma_r$ ,  $n_r^{\alpha\beta\text{cis}}$ , and  $n_r^{\beta\beta\text{cis}}$  are readily found by simple inspection. The results are given in table I.

We assume that the interactions between neighboring *o*-tolyl rings are more repulsive in the cis than in the trans configuration, i.e.,  $G^{\beta\beta\text{cis}} - G^{\beta\beta\text{trans}} > 0$  and  $G^{\alpha\beta\text{cis}} - G^{\alpha\beta\text{trans}} > 0$ . We obtain  $0 < y < 1$  and  $0 < z < 1$  and establish the following ordering of the rotamer populations from their algebraic expression (Table I) whatever the relative values of  $z$  and  $y$ :

$$\begin{aligned} x_1 &< x_2 < x_5 \\ x_1 &< x_3 < x_6 \\ x_1 &< x_4 < x_6 \\ x_1 &< x_4 < x_5 \end{aligned} \quad (3)$$

From the inequalities in eq 3, it results that rotamer  $I_1$  is the least populated one, as expected, since it is the most sterically crowded one, with its four methyl groups on the same side of the central ring. Therefore, the two small, equally intense signals  $6\beta$  and  $9\alpha$  are assigned to rotamer  $I_1$ .

The  $\alpha^1$  and  $\beta^1$  submatrices of the 2D spectrum show that signal  $9\alpha$  correlates with signals  $2\alpha$  and  $16\alpha$  while signal  $6\beta$  correlates with signals  $8\beta$  and  $11\beta$ . If we assume that indeed the mode  $M_1$  proceeds, (see Figures 8 and 9 of ref 4), the signals 2, 8, 11, and

(10) Haywood-Farmer, J.; Battiste, M. A. *Chem. Ind. (London)* **1971**, 1232.

(11) Pepermans, H., unpublished results.

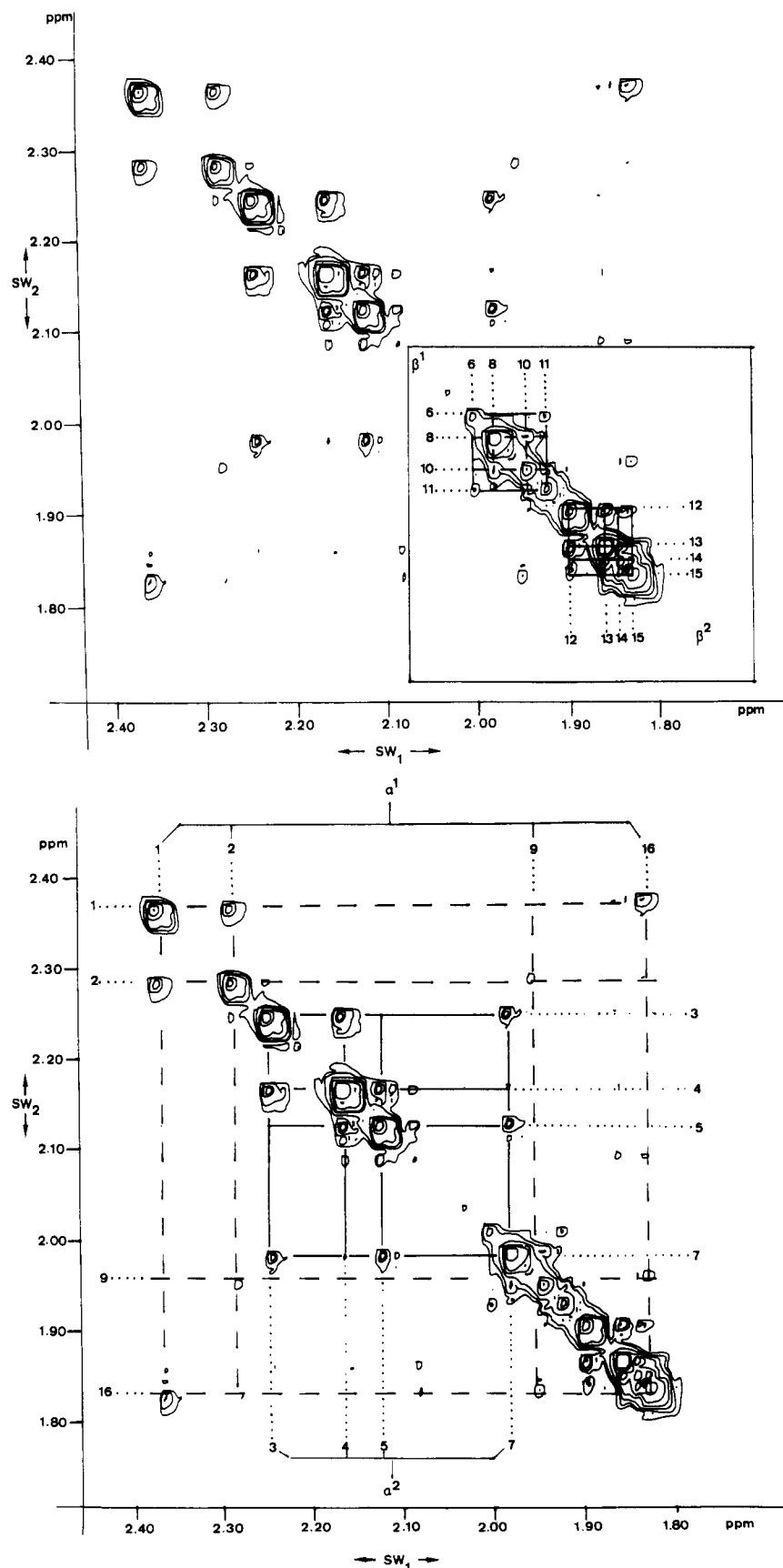


**Figure 2.** Slow-exchange EXSY 2D spectrum at 500 MHz at 1, in the methyl region, at  $-43^\circ\text{C}$  in  $\text{CDCl}_3$ : (A) exchange of  $\alpha$  methyl signals, (B) exchange of  $\beta$  methyl signals. In these spectra, the main diagonal goes unusually from the top left to the bottom right in order for these 2D spectra to have the same aspect as the magnetic site exchange matrices of which they are a faithful representation.

16 are assigned to the pair of rotamers  $I_2/I_3$ ; the spectrum of Figure 4 in ref 4 confirms that the signals 2, 11, and 16 have reasonably equal intensities while signal 8 overlaps with signal

7. Because the signals  $2\alpha$  and  $16\alpha$  and  $8\beta$  and  $11\beta$  correlate with the signals  $1\alpha$  and  $10\beta$ , respectively, these are assigned to the rotamer  $I_3$ . The spectra of Figure 1 and of Figure 4 of ref 4

confirms that the resonances 1 and 10 have reasonably equal intensities. Starting, on the other hand, from the fact that the pair of rotamers  $I_6/I_8$  has the highest population among those with only two resonances as shown by the inequalities of (3), we assign the resonances  $4\alpha$  and  $13\beta$  to this pair. An argumentation, similar to that above, leads to an assignment of signals  $3\alpha$  and  $5\alpha$  and  $12\beta$  and  $14\beta$  to the pair of rotamers  $I_5/I_3$  and the resonances  $7\alpha$  and  $15\beta$  to  $I_4/I_2$ .

The signal assignment (see Table I) being now achieved, we are able to estimate the experimental rotamer population from the spectrum of Figure 4 of ref 4. To do so, we calculated the surfaces of the triangulated signals of an expansion of this spectrum and computed the population of rotamer  $r$  by dividing the sum of the surfaces of the signals associated with rotamer  $r$  by the sum of all the signal areas. The populations are given in Table I as  $x_r^{\text{exptl}}$ . We checked then the self-consistency of the rotamer assignment with the choice of  $M_1$  by minimizing the function numerically:

$$F = \sum_{r=1}^6 (x_r^{\text{exptl}} - x_r^{\text{calcd}})^2 \quad (4)$$

The function  $F$  has the minimum value of  $2.88 \times 10^{-3}$  when  $z = 0.617$  and  $y = 0.539$ , which correspond with the values of  $G^{\alpha\beta\text{cis}} - G^{\alpha\beta\text{trans}} = 0.22$  kcal/mol and  $G^{\beta\beta\text{cis}} - G^{\beta\beta\text{trans}} = 0.29$  kcal/mol at  $-40^\circ\text{C}$ , revealing that the  $\beta\beta$  interaction is sterically more demanding than the  $\alpha\beta$ . Using the numerical values of  $z$  and  $y$  above, we calculated the rotamer populations using eq 2 and the data of Table I. The results, also given in this table, show that the agreement between the experimental rotamer populations and those calculated for  $M_1$  is fairly good.

If we assume, on the other hand, the assignment resulting from mode  $M_2$ , i.e., when  $I_2/I_3$  and  $I_5/I_3$  are permuted (see Figures 8 and 9 of ref 4), the minimum value of  $F$  is about 8 times larger than the value found for  $M_1$ , and the agreement between experimental and calculated populations is poor (see Table I).

Moreover, the  $\alpha\beta$  interaction appears to be more repulsive ( $z = 0.60$ ;  $G^{\alpha\beta\text{cis}} - G^{\alpha\beta\text{trans}} = 0.24$  kcal/mol) than the  $\beta\beta$  one ( $y = 0.94$ ;  $G^{\beta\beta\text{cis}} - G^{\beta\beta\text{trans}} = 0.03$  kcal/mol). This would in turn mean that the  $\alpha$  *o*-tolyl ring is more sterically hindered than the  $\beta$  one, which is very unlikely. We can, therefore, conclude that only the rotamer assignment which was derived with the  $\alpha$  one ring rotation  $M_1$  as the threshold mode leads to self-consistent results.

As a consequence of this assignment, the residual  $\beta$  signals at  $30^\circ$  (Figure 3 or ref 4) can now also be attributed more precisely. The one at 1.99 ppm results from the averaging of  $\beta$  signals of  $I_1$ ,  $I_2/I_3$  and  $I_3$ , which have in common that the  $\beta$  methyl groups lie cis to one another. In contrast, the  $\beta$  residual signal at 1.88 ppm is associated with  $\beta$  methyls in trans to one another.

This allows a further assignment of the two signals of 3,4-di-*o*-tolyl-2,5-diphenylcyclopentadienone<sup>10</sup> to the cis rotamer at 2.04 ppm and to the trans rotamer at 1.90 ppm.

In conclusion, this work shows unambiguously that 2D NMR spectroscopy, albeit in conjunction with its 1D counterpart, allows to get a much more precise insight into both the static and dynamic stereochemistry of **1**. The complete rotamer assignment and the more precise evidence for the  $\alpha$  one ring rotation as the threshold mode show this undoubtedly.

### Experimental Section

The characteristics of compound **1** are given elsewhere.<sup>4</sup> The 2D spectra were recorded at 230 K on a Bruker AM 500 spectrometer, equipped with an aspect 3000 computer and a B-VT 1000 temperature unit. For the exchange experiment a sequence of three pulses,  $[90^\circ - t_1 - 90^\circ - \tau_m - 90^\circ - t_2]_n$  was used where  $\tau_m$  is the so-called mixing time. For this experiment 64 FID'S (of 64 scans each consisting of 512w data points) were accumulated, after digital filtering sine bell; the FID was zero-filled to 256w in the  $F_1$  dimension. Fourier transformation yielded a spectrum with 1.95 Hz/point digital resolution in both dimensions. Typical acquisition parameters were  $sw_1 = \pm 250$  Hz,  $sw_2 = 500$  Hz,  $\Delta t_1 = 0.2$  ms, 1.5-s recycle delay, and  $\tau_m = 80$  ms.

Registry No. **1**, 77243-07-3.

## <sup>13</sup>C and <sup>1</sup>H EPR Analysis of the Benzo[*a*]pyrene Cation Radical

Paul D. Sullivan,\*† Fouad Bannoura,† and Guido H. Daub‡

Contribution from the Departments of Chemistry, Ohio University, Athens, Ohio 45701, and the University of New Mexico, Albuquerque, New Mexico 87131. Received June 25, 1984

**Abstract:** The <sup>13</sup>C splittings for benzo[*a*]pyrene (BaP) cation radicals singly labeled at each protonated position have been determined by measuring the increase in the total width of the EPR spectrum of the <sup>13</sup>C derivatives over that of the unlabeled parent molecule. The absolute values of the <sup>13</sup>C splittings found for the 12 protonated positions (1-12, respectively) are 6.01, 4.55, 4.44, 0.93, 1.32, 8.30, 3.74, 2.91, 3.01, 1.29, 1.96, and 3.60 G. Additionally, with the aid of deuterated BaP and by comparison with computer simulations, an analysis is proposed for the proton splittings in BaP<sup>+</sup> in terms of the following 12 splitting constants for positions 1-12, respectively, 4.57, 0.54, 3.77, 0.37, 2.11, 6.63, 2.23, 0.19, 2.95, 1.94, 0.82, and 2.75 G. When the Karplus-Fraenkel theory for <sup>13</sup>C splittings is used, the results are compared for internal consistency with those previously estimated from the methylated BaP's. Several deviations from calculated values have been found which may have some significance to the metabolism of BaP and its derivatives.

The electron paramagnetic resonance (EPR) spectrum of the benzo[*a*]pyrene (BaP) cation radical was first observed over 25 years ago<sup>1</sup> and has since been investigated by several groups<sup>2-4</sup> but has so far resisted complete analysis. The analysis of the EPR spectrum is important because of the information it would provide regarding the spin density distribution in the highest occupied

molecular orbital (HOMO) of the BaP molecule. Such knowledge would be useful in the correlation of molecular parameters with metabolic products<sup>5,6</sup> as well as regards the speculation that cation

\* Ohio University.

† University of New Mexico. Deceased June 1984.

(1) Kon, H.; Blois, M. S. *J. Chem. Phys.* **1958**, *28*, 743-744.

(2) Nagata, C.; Inomata, M.; Tagashira, Y. *Gann* **1968**, *59*, 289-298.

(3) Forbes, W. F.; Robinson, J. C.; Wright, G. V. *Can. J. Biochem.* **1967**, *45*, 1087-1098.

(4) Elmore, J. J.; Forman, A. *Cancer Biochem. Biophys.* **1975**, *1*, 115-120.